Review Article

JHS(E)

Journal of Hand Surgery
(European Volume)
2025, Vol. 50(6) 771–780

DOI: 10.1177/17531934251327286
journals.sagepub.com/home/jhs
Sage

The Role of 3D technology in corrective osteotomy for forearm malunion

Pieter Reyniers[1,2], Dries Verrewaere[1,3], Eline van Es[4], Joost Colaris[4], Andreas Schweizer[5] and Frederik Verstreken[1,6]

Abstract

Forearm malunion affects upper limb function, impairing rotation, grip strength, and dexterity. Traditional osteotomies, based on two-dimensional imaging and intraoperative adjustments, may fail to address the intricate three-dimensional aspects of forearm deformities. Advances in 3D technology, including imaging, virtual surgical planning and 3D-printed patient-specific guides, have transformed corrective osteotomy by enhancing precision and predictability. This paper discusses the limitations of traditional methods, the role of 3D imaging in detailed deformity analysis, the benefits of virtual planning and the use of 3D surgical guides to improve outcomes. The use of 3D technology in both paediatric and adult cases is illustrated in a supplementary series of case reports. Future improvements in artificial intelligence, robotics and augmented reality are expected to enhance 3D-guided osteotomies further, making them more accessible and cost-effective.

Keywords

3D technology, corrective osteotomy, forearm malunion, functional anatomy, patient-specific guides

Date received: 20th January 2025; revised: 18th February 2025; accepted: 26th February 2025

Introduction

Forearm fractures are common orthopaedic injuries, with malunion their most frequent complication. Malunion can impact upper limb function considerably, particularly forearm rotation, grip strength and overall dexterity. The radius and ulna function as a single unit to support motion and load transmission, requiring anatomical alignment for optimal function.

Conventional osteotomies for managing forearm malunion rely on planning based on two-dimensional (2D) radiographs, overlay drafting, freehand osteotomies and fluoroscopy guidance (Jupiter et al., 1992). However, these methods fail to adequately represent the three-dimensional (3D) complexity of the deformities, often a combination of angular deformity, malrotation and translation (Ries and O'Neill, 1987). Surgical correction and fixation have traditionally depended on intraoperative trial-and-error approaches, guided by fluoroscopic imaging and the experience of the surgeon. While these methods have achieved satisfactory outcomes in many cases, they are inherently limited by their reliance on subjective assessment and a lack of precision, often resulting in suboptimal corrections (von Campe et al., 2006).

Recent advances in 3D technology have substantially improved the evaluation and treatment of forearm malunion (Murase et al., 2008). Three-dimensional imaging enables a more comprehensive assessment of the deformity, accurately capturing the combination of angular, rotational and translational components. The computer can detect and analyse a deformity, which even the most experienced surgeon may not be able to identify. With 3D

[1]AZ Monica, Antwerp, Belgium
[2]VITAZ, Sint Niklaas, Belgium
[3]AZ Sint-Jan, Brugge, Belgium
[4]Erasmus University Medical Centre, Rotterdam, The Netherlands
[5]Balgrist University Hospital, Zürich, Switzerland
[6]University of Antwerp, Antwerp, Belgium

Corresponding Author:
Frederik Verstreken, AZ Monica, Florent Pauwelslei 1, 2100 Antwerp, Belgium.
Email: frederik.verstreken@live.com

planning, surgeons can simulate corrective osteotomies and rehearse surgical strategies virtually, improving preoperative decision-making. The advent of patient-specific, 3D-printed surgical guides allows for precise execution of planned corrections, reducing intraoperative uncertainty and improving outcomes.

This paper provides an overview of the functional anatomy and clinical implications of forearm malunion, examining the evolving role of 3D technology.

Functional anatomy and malunion

Understanding the biomechanics of the forearm and the radioulnar joints begins with the osteology of the radius and ulna. The ulna has a sigmoid curvature in the coronal plane, with a radial apex proximally and an ulnar apex distally (Beşer et al., 2014; Hreha et al., 2020; Weber et al., 2020). The proximal ulna has a dorsal angulation, known as proximal ulnar dorsal angulation, which it is important to restore in proximal ulnar fractures (Rouleau et al., 2010) (Figure 1).

The radius bows radially in the coronal plane to allow rotation around the ulna, with the apex located at its middle third (Rupasinghe and Poon, 2012; Weber et al., 2020). In the sagittal plane, the radius exhibits an apex dorsal bow. In terms of rotation, the bicipital tuberosity is positioned roughly 180° opposite the radial styloid. However, the tuberosity's bulbous shape can complicate the precise radiographic identification of its most prominent point.

The radius and ulna articulate at both ends with a condylar pivot joint, and the forearm functions as a single joint, with the radius rotating around the stable ulna, with the axis extending from the central radial head to the ulnar head's fovea. Any fracture of the radius or ulna can essentially be considered 'intra-articular' as the integrity of the radioulnar joint is critical for forearm rotation, which covers approximately 160° in a nearly circular arc.

The stability of the forearm or radioulnar joint relies on the bone and joint architecture, and on three structures: the annular ligament, interosseous membrane (IOM), and triangular fibrocartilage complex (TFCC) (Robinson and Shatford, 2021). Together, these elements ensure consistent tension between the radius and ulna, enabling stable and full rotational movements during pronation and supination (Video 1, 2).

The ulna translates by 9° in the coronal plane as the radius rotates. During pronation, contraction of the anconeus causes the ulna to abduct, while in supination, the ulna adducts relative to the humerus. This dynamic motion ensures that the axis of rotation consistently aligns with the middle finger (Barton and Evans, 1991; Hreha et al., 2020). The radius migrates slightly proximally in pronation, creating a relative lengthening of the ulna (positive ulnar variance). Additionally, the ulnar head shifts dorsally in pronation, a phenomenon that becomes more pronounced under axial loading (Cerezal et al., 2002). From a practical perspective, axial views on CT or

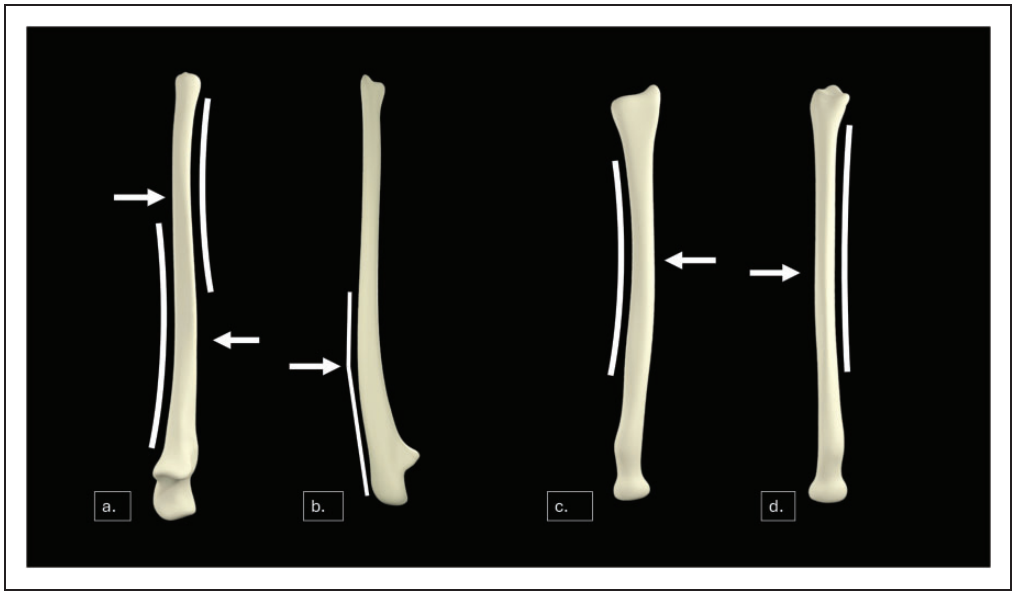

Figure 1. (a) Anteroposterior (AP) view of the ulna, demonstrating its characteristic sigmoidal shape with a proximal radial apex and a distal ulnar apex. (b) Lateral view of the ulna illustrating the proximal ulnar dorsal angulation (PUDA). (c) Anteroposterior view of the radius, highlighting the radial bow in the middle third of the bone and (d) lateral view of the radius showing a subtle dorsal apex bow.

MRI scan reveal the forearm's rotational position; in supination, Lister's tubercle moves towards the ulnar styloid, and in pronation is moves away (King et al., 1986).

Clinical implications

Forearm malunion can impair upper limb function and quality of life by restricting rotation, reducing grip strength and impairing load transmission (Trousdale and Linscheid, 1995). Malunion can also cause pain and instability between the radius and ulna, with consequent loss of function (Chia et al., 2011; Trousdale and Linscheid, 1995). Secondary complications, such as joint degeneration, muscle imbalances and nerve compression syndromes, are common and further impair function (Bauer et al., 2017). Moreover, malunion can affect cosmetic appearance, which, particularly in children, may lead to mental health challenges owing to feeling different from their peers (Trousdale and Linscheid, 1995).

Malunions are typically multiplanar relative to anatomical alignment, and angulation or rotation exceeding 10° can result in substantial restrictions in movement (Matthews et al., 1982; Tarr et al., 1984). A malunited fracture of the radius in a growing skeleton can misdirect ulnar growth, potentially resulting in a situation where both bones require correction later to restore optimal function (Colaris et al., 2014a; Furrer et al., 2023; Graham et al., 1998).

Restriction of pronation is often caused by bony impingement in the proximal forearm, where the radius and ulna have minimal clearance, typically only a few millimetres (Christensen et al., 1968) (Figure 2). Such deformities often result from untreated or poorly managed proximal or middle third radial shaft fractures (Fuller and McCullough, 1982; Matthews et al., 1982). These fractures frequently heal with an extension deformity, increasing the risk of impingement and restricted pronation (Shiode et al., 2024). A rotational deformity of the radial shaft can result in loss of pronation, and malrotation in one direction leads to an equivalent loss of forearm rotation in the opposite direction (Tarr et al., 1984). Fractures distal to the pronator teres insertion produce supinate of the distal fragment from muscle forces. (Dumont et al., 2002; Kasten et al., 2003; Mania et al., 2023).

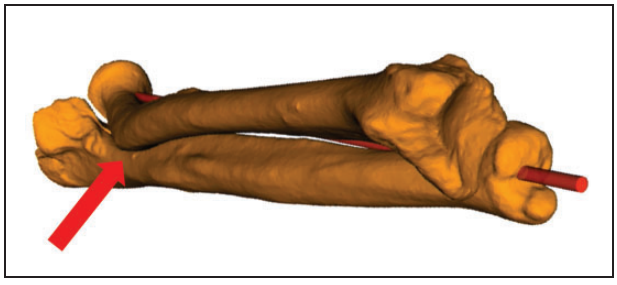

Figure 2. Impingement of a malunited radius onto the ulna limiting pronation.

Supination restriction is typically caused by radial shaft fractures that heal with a flexion deformity, causing increased tension in the IOM. In a normal forearm, the origin of the central band on the radius and its insertion to the ulna are near the rotational axis, allowing the IOM's tension and length to increase by only about 0.5 mm from neutral to maximal supination. Malunion can displace these insertional points away from the rotational axis and their isometric position, resulting in excessive tension on the IOM and restricting supination (Moritomo et al., 2009; Noda et al., 2009). Additionally, radial shaft fractures between the insertions of the biceps or supinator and pronator teres muscles produces muscle forces, resulting in pronation of the distal fragment, limiting supination (Dumont et al., 2002; Kasten et al., 2003).

Instability at the distal radioulnar joint (DRUJ) is a common consequence of malunion (Trousdale and Linscheid, 1995) (Figure 3, Video 3). Palmar dislocation of the ulnar head relative to the radius (or dorsal displacement of the radius relative to the ulna), particularly at the end of supination, is often caused by a mild extension deformity of the radius shaft (Schmitt et al., 2023). This deformity can be subtle and difficult to detect on conventional radiographs. Clinically, it presents as a snapping sensation at the end of supination, when the ulnar head shifts out of the sigmoid notch in a palmar direction. Pronation repositions the joint through the pull of the IOM (Nagy et al., 2008). Over time, instability can lead to ligament laxity or TFCC degeneration, further compounding the condition. Patients with relative ligamentous laxity or hypermobility are prone to developing an unstable DRUJ, while those with stiffer connective tissue tend to experience a restricted range of motion. Correcting the malunion will usually stabilize the DRUJ through its secondary stabilizers, such as the distal oblique bundle of the IOM (Schmitt et al., 2023). Conversely, a flexion deformity in a radial shaft malunion can cause excessive dorsal translation of the ulnar head, resulting in a painful DRUJ. Addressing this uncommon malunion pattern can often resolve the issue without requiring soft tissue intervention (Nishiwaki et al., 2015) .

Persistent dislocation of the radial head in the proximal radioulnar joint presents a more complex challenge and is frequently associated with ulnar malunion. These cases, often linked to missed Monteggia

Figure 3. Malunion with distal radioulnar joint instability.

lesions, may require extensive intra-articular debridement and annular ligament reconstruction, combined with an ulna osteotomy to stabilize of the radial head and restore function (Langenberg et al., 2020).

Paediatric patients generally tolerate malunion better owing to joint laxity and the potential for skeletal remodelling (although this depends on age, location and degree of deformity (Carey et al., 1992; Fuller and McCullough, 1982). Children with diaphyseal both-bone forearm fractures face a moderate risk (13–33%) of functional limitation, regardless of the severity of the angular malalignment (Colaris et al., 2014b). Price and Knapp (2006) advised performing corrective osteotomy for forearm shaft malunions as soon as possible when angulations exceed 30°, while recommending a waiting period of at least 6 months for malunions with angulations between 20° and 30°. However, delayed surgery beyond 1 year is associated with poorer outcomes owing to secondary joint and soft-tissue alterations (Roth et al., 2017).

Basics of 3D planned correction (Video 4)

The most effective way to analyse a forearm malunion is by using a mirrored model of the contralateral normal side. Cross-sectional bilateral high-resolution CT images are processed using segmentation software to isolate the bone. Whenever possible, both forearms should be scanned simultaneously to minimize radiation exposure. If an additional scan of the contralateral arm is necessary, a low-dose protocol (approximately 0.2 mSv) can be used, although maintaining a slice thickness of $\leq$0.6 mm is needed to ensure high-resolution imaging. To isolate bones from other tissue, cross-sectional CT images are processed with segmentation software (Belvedere et al., 2022).

The next step is to separately match the radius and ulna from the affected and mirrored unaffected sides. The proximal part of both bones is aligned using iterative closest point surface-based registration. Similarly, the distal alignment is achieved using a duplicate of the mirrored side, creating a comprehensive model of the location, degree and type of malunion.

The relative positions of the proximal and distal bone segments in a forearm malunion define the deformity and the planned correction. Often a single-plane rotational osteotomy can address the malalignment effectively with the osteotomy plane oriented perpendicular (normal) to a single rotational axis (Sangeorzan et al., 1989). This ‘single cut’ technique offers several advantages. Firstly, it is precise, requiring only one well-defined osteotomy plane. Secondly, repositioning is simplified: the distal fragment is rotated around the chosen axis to the correct alignment. Thirdly, this approach maximizes the surface area for bony contact, allowing the use of an interfragmentary compression screw, enhancing stability after fixation (Figure 4).

Some deformities, however, are better managed with an opening or closing wedge osteotomy. These are useful if additional adjustment of length or translation is required, or if the angular deformity is too great to be adequately corrected by rotation alone (Figure 5). In such cases, careful planning is needed to ensure proper realignment, restoration of forearm length and ulnar variance, and stable osteosynthesis, sometimes necessitating bone grafting or different fixation constructs.

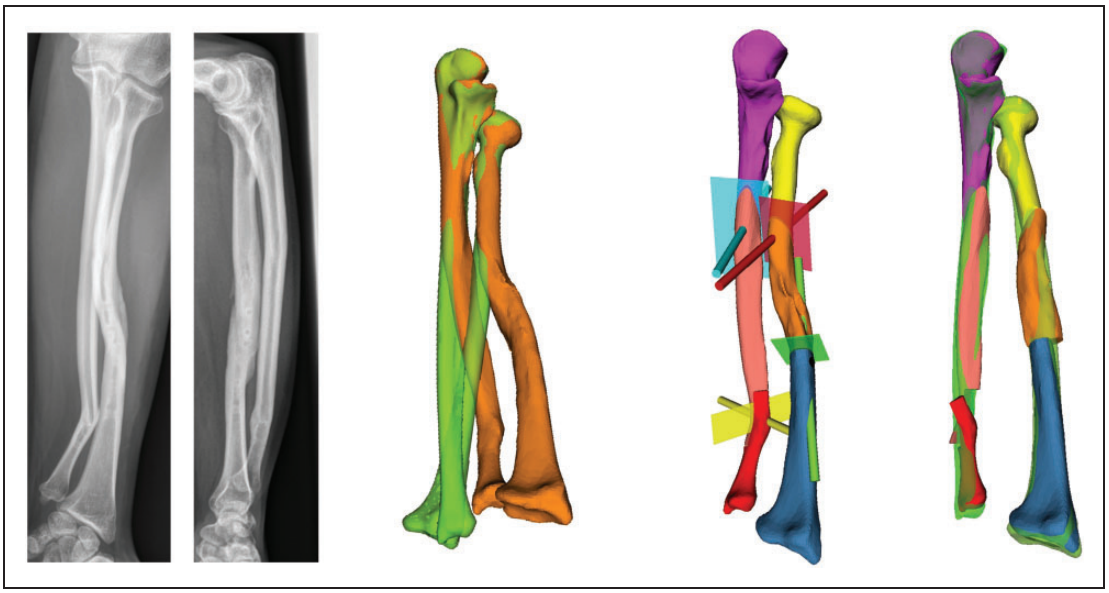

Figure 4. Multilevel corrections with single-plane rotational osteotomies, oriented perpendicular (normal) to the rotational axis.

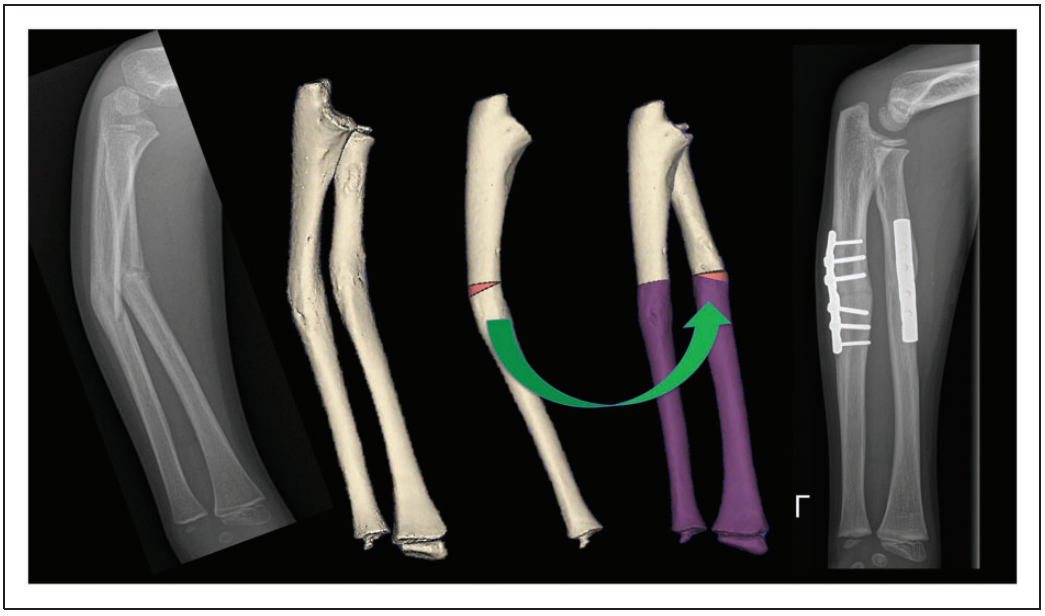

Figure 5. Closing wedge osteotomy of the ulna combined with an opening wedge osteotomy of the radius, using the resected ulnar wedge as a bone graft.

Nowadays, many commercial software solutions, such as Mimics and 3-Matic (Materialise NV, Leuven, Belgium) and CASPA (Balgrist CARD, Zurich, Switzerland), provide tools to facilitate calculations and simulate the correction aimed at restoring both proximal and distal alignment.

After planning the optimal correction, the position of the plate (2.5–3.5 mm) must be determined. This requires consideration of possible surgical approaches, the presence of soft tissue attachments and identification of a flat surface on the bone. Computer-assisted planning relies on bony anatomy, while soft tissues may interfere with precise guide placement. For the technical feasibility of the plan, close cooperation between the surgeon and the engineer is essential. General surgical tips for using surgical guides in forearm corrections are outlined in Table 1.

To improve the accuracy of a planned correction, patient-specific guides can be designed and 3D

printed. This involves reverse engineering, where the postoperative screw position is used to calculate to their preoperative position on the bone. To ensure rotational stability, at least two locking screws on each side of the osteotomy are planned. If possible, the cutting sleeve(s) for the osteotomy can be incorporated into the same guide, otherwise a second guide must be designed. In this case, two parallel K-wires on each guide ensure identical positioning on the bone. Guides should be printed using biocompatible and sterilizable materials, such as PA12 or resin to minimize the risk of infection.

Accurate guide positioning on the bone is essential, so distinct anatomical features of the bone within the contact surface area of the guide are included to ensure precise positioning. By 3D printing the preoperative bone model, marking the borders of the guide(s) on it, and by printing the guide twice, the correct position can be verified intraoperatively by comparing guide position and K-wire position on the model and the patient under fluoroscopy (Figure 6). The proximal–distal orientation can also be verified by comparing measurements from the radial head and ulnar styloid between the patient and the model.

When standard fixation plates do not conform well to the bony contours, they can be pre-shaped on pre-printed models of the corrected bones. These adapted plates are then scanned and used to design a surgical guide. A more advanced but costly alternative is the design and fabrication of patient-specific implants (PSIs), which provide customized fixation solutions tailored to the patient's unique anatomy and biomechanics. These implants ensure an exact fit, which facilitates reduction of bony fragments and provides rigid, stable fixation. This level of precision enhances surgical outcomes and minimizes the risk of complications associated with improper alignment.

Corrective osteotomy as a revision procedure tends to be more complex owing to dense scar tissue, fibrosis and altered anatomy. In addition, the bone may be weakened by stress shielding caused by

Table 1. General surgical tips when using surgical guides in forearm corrections

Obtain adequate exposure	Make sure you have complete visualization of the osteotomy site. Be aware that the segmentation is based on the exact bone contours, not on the periosteum or other interposing soft tissues. This helps ensure the guide fits securely and accurately
Maintain visual control	Once the guide is in place, it can be difficult to see the underlying structures. Always maintain direct visualization and protect surrounding soft tissues with retractors, especially around the cutting sleeve
Secure the guide firmly	Relying solely on K-wires to stabilize the guide can be insufficient. Use additional bone clamps as needed to achieve stable fixation and prevent guide movement during cutting
Use intraoperative cooling	Incorporate cooling measures during osteotomies to avoid heat-induced bone necrosis, as 50°C for 30 s is the critical limit for heat-induced bone necrosis, potentially affecting union (Lundskog, 1972)

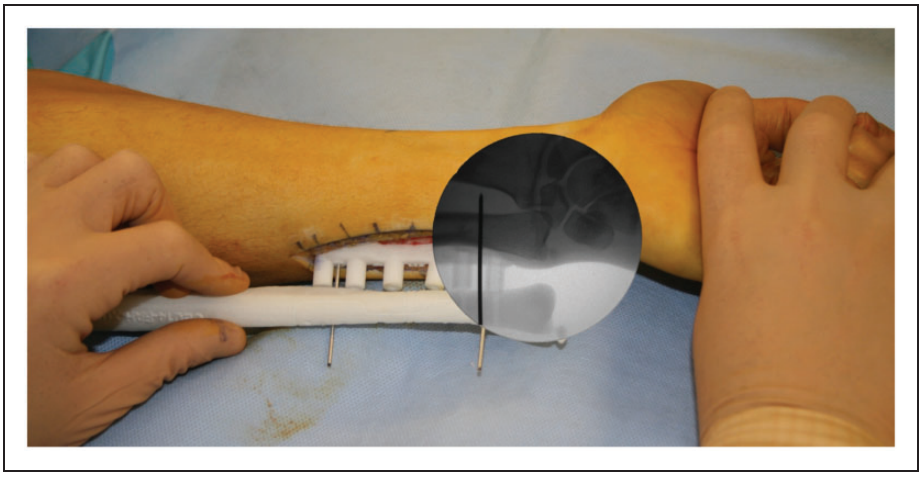

Figure 6. The correct position of the guide can be verified intraoperatively by comparing guide position and K-wire position on the printed bone model and the patient under fluoroscopy.

the original plate or by existing screw holes that act as stress risers. These factors increase the technical difficulty of the procedure and complication rate, including neurovascular injury and postoperative stiffness. The pre-existing plate footprint can be advantageous by providing a reference for designing the surgical guide, thereby facilitating accurate placement (Figure 7). Existing screw holes can also be reused both to temporarily secure the guide and for subsequent bony fixation, reducing the need for additional drilling and helping to preserve bone integrity.

Discussion

In the early 2000s, CT imaging and specialized software began to influence preoperative planning by enabling virtual surgical plans that detailed osteotomy sites, plate positioning and rotational corrections. Croitoru et al. (2001) advanced this concept by introducing a guide system based on anatomical landmarks. While 3D-printed fracture models were initially limited to preoperative planning owing to high production costs, advances in 3D printing during the 2010s made patient-specific surgical guides both feasible and cost-effective (Jupiter et al., 1992; Miyake et al., 2012). The radiographic accuracy of published series is summarized in Table 2. The improved accuracy of 3D-guided techniques is reflected in postoperative radiographic outcomes, which consistently outperform those of traditional methods (Buijze et al., 2018; Vlachopoulos et al., 2015; Vroemen et al., 2013).

The advantages of 3D-assisted surgery extend beyond accuracy. Reduced reliance on fluoroscopy lowers radiation exposure for both the surgical team and the patient. The enhanced preoperative assessment of bone geometry ensures proper screw placement and reduces the risk of screw protrusion shortening surgical time and lowering complication rates from 12% using conventional techniques to 6%. (Buijze et al., 2018; Bauer et al., 2017; Meesters et al., 2024).

Functional outcomes are also superior with 3D-assisted surgery. Most studies report better range of motion and greater improvements in functional scores. For instance, the median Disabilities of the Arm, Shoulder and Hand score improves by an average of 35 (SD 5) in 3D-guided cases, compared with 28 (SD 7) in conventional surgery (Meesters et al., 2024). These findings highlight the importance of precise anatomical correction in achieving optimal functional outcomes (Kataoka et al., 2018; Miyake et al., 2012; Roth et al., 2022).

Challenges and limitations of 3D methods

While 3D methods significantly enhance surgical precision, they require training and time investment,

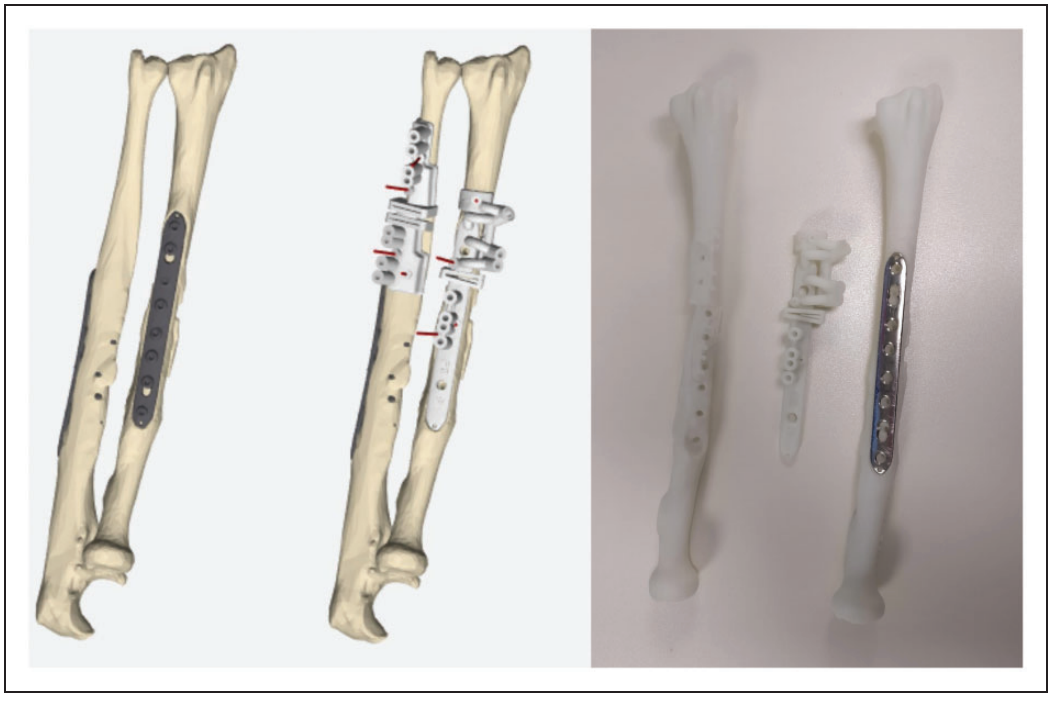

Figure 7. In revision cases, the footprint of the pre-existing plate can be used as a template for guide design, thereby facilitating accurate placement.

Table 2. Postoperative accuracy in corrective osteotomy for radial and/or ulnar shaft malunions using surgical guides

Study	Patients	Average postoperative residual angle of deformity	Postoperative radiologic evaluation
Murase et al. (2008)	4 radius, 1 ulna, 5 radius and ulna	0.7° (range 0–3°)	Radiographs, compared with the contralateral forearm
Miyake et al. (2012)	14 radius and ulna, 6 radius	1° (range 0–4°)	Radiographs, compared with the contralateral forearm
Kataoka et al. (2018)	3 radius and ulna, 1 radius	<2.7°, with exclusion of 1 case with double opening wedge osteotomy and increase in deformity because of longitudinal growth	CT-scan, compared with the preoperative plan
Byrne et al. (2017)	5 radius and ulna	1.8° (range 0.3–5.2°) for the ulna and 1.4° (range 0.2–3.3°)	Radiographs, compared with the contralateral forearm
Roner et al. (2017)	6 radius, 6 ulna	5.8° (SD 3.6°) true deformity angle	CT-scan, compared with the preoperative plan
Oka et al. (2019)	1 radius and ulna, 2 radius	3.2° (SD 1.4°) true deformity angle	Radiographs, compared with the contralateral forearm. True deformity angle was calculated
Roth et al. (2022)	15 radius and ulna	2.6° (SD 3.1°) for the radius and 1.7° (SD 1.7°) for ulna. Residual rotational deformity was measured separately and was 6.6° (SD 4.8°) for the radius and 5.5° (SD 5.3°) for the ulna	CT scan, compared with the preoperative plan

with associated cost. Expenses include CT scanning, software licences, and 3D printers, but also the work hours required from engineers and technicians. In the future, increased competition among software providers may help drive down these costs. Currently, outsourcing 3D planning and printing for surgical guides can cost between €2000 and €3500 per case, depending on the complexity of the deformity, with an additional €1500 possible for printing custom implants. Another barrier is the learning curve for surgeons adopting 3D tools. Without adequate training and integration into clinical workflows, these technologies run the risk of being underutilized. Time expenditure in preoperative planning also poses a limitation, as creating and validating 3D models requires several extra steps beyond traditional methods – typically 2–4 hours, depending on case complexity. However, automation and more intuitive software interfaces continue to improve efficiency in this area. Lastly, an over-reliance on 3D technology may erode essential surgical skills if not balanced with traditional techniques. Three-dimensional methods should be seen as tools to enhance surgical expertise, rather than replace it. By combining technological advancements with clinical acumen, surgeons can maximize patient outcomes while maintaining core competencies.

Ethical and economic considerations

Since their introduction in the 2010s, 3D-printed surgical guides have improved surgical accuracy, radiographic outcomes and functional outcomes for patients compared with conventional techniques. Despite these advantages, the cost of implementing 3D-printed guides has limited their widespread use worldwide. In resource-limited settings, financial constraints often require the prioritizing of essential healthcare services over the adoption of newer, more expensive technologies. However, where computer infrastructure is available and low-cost, open-source software and basic 3D printers are paired with proper training, these technologies could become more accessible without compromising more urgent healthcare priorities.

Ethically, providers should balance the immediate costs against the broader value of adopting cutting-edge technologies that can improve patient outcomes.

Future directions and innovations

The integration of 3D printing technologies with others such as artificial intelligence, robotics, and augmented reality (AR) may radically transform clinical practice. Artificial intelligence can automate segmentation deformity definition, plate positioning using statistical shape models, screw placement

based on CT-derived bone density, and specific implants customisation Carrillo et al. (2020). Advances in robotic-assisted techniques may further refine malunion correction, using cold ablation and robot-guided laser osteotomies, minimizing thermal damage whilst maintaining accuracy (Honigmann et al., 2022). Meanwhile, AR headsets can project 3D anatomical models directly into the surgical field, enabling surgeons to maintain visual focus and enhance procedural accuracy (Dennler et al., 2021; Lex et al., 2023). In the future, AR may replace physical guides and reduce the need for 3D-printed components, ultimately lowering costs. By integrating these cutting-edge technologies with current 3D-printing workflows, hand surgery may become more efficient, precise and cost-effective, improving patient outcomes and redefining standards of care.

The use of 3D technology into corrective forearm osteotomy for forearm malunion represents a considerable advancement in treating these complex problems. Despite clear advantages in terms of accuracy and reduced complications, the widespread adoption of 3D technology remains limited by the resources required. Looking ahead, emerging solutions in artificial intelligence, robotics and augmented reality promise to further refine osteotomy planning, potentially eliminating the need for physical guides and making sophisticated interventions more accessible. As the field evolves, 3D technology is likely to become a cornerstone of forearm corrective surgery, bridging the gap between traditional techniques and cutting-edge innovations.

Acknowledgements Not applicable.

Author contributions FV contributed to the development of the structure and outline. All authors collaborated on the initial draft of the manuscript and participated in its review and editing. PR and FV conducted the final review, and all authors approved the final version of the manuscript.

Declaration of conflicting interests Frederik Verstreken receives royalties from Materialise. Andreas Schweizer is a co-founder former CARD AG, my-osteotomy (Medacta SA).

Ethical approval Not applicable

Funding The author(s) received no financial support for the research, authorship, and/or publication of this article.

Informed consent All procedures were in accordance with the Helsinki declaration of 1975, as revised in 2008. Informed consent was obtained for all patients in this study.

ORCID iD Frederik Verstreken https://orcid.org/0000-0003-2849-1190

Supplementary material Supplemental material for this article is available online.

References

Barton BA, Evans EJ. Movements of the elbow and shoulder during pronation of the forearm. Clinical Anatomy. 1991, 4: 421–32.

Bauer DE, Zimmermann S, Aichmair A et al. Conventional versus computer-assisted corrective osteotomy of the forearm: a retrospective analysis of 56 consecutive cases. J Hand Surg Am. 2017, 42: 447–55.

Belvedere C, Ortolani M, Marcelli E et al. Comparison of bone segmentation software over different anatomical parts. Appl Sci. 2022, 12: 6097.

Buijze GA, Leong NL, Stockmans F et al. Three-dimensional compared with two-dimensional preoperative planning of corrective osteotomy for extra-articular distal radial malunion: a multicenter randomized controlled trial. J Bone Joint Surg Am. 2018, 100: 1191–202.

Beşer CG, Demiryürek D, Özsoy H et al. Redefining the proximal ulna anatomy. Surg Radiol Anat. 2014, 36: 1023–31.

Byrne AM, Impelmans B, Bertrand V, Van Haver A, Verstreken F. Corrective osteotomy for malunited diaphyseal forearm fractures using preoperative 3-dimensional planning and patient-specific surgical guides and implants. J Hand Surg Am. 2017, 42: 836.e1–e12.

Carey PJ, Alburger PD, Betz RR, Clancy M, Steel HH. Both-bone forearm fractures in children. Orthopedics. 1992, 15: 1015–9.

Carrillo F, Roner S, von Atzigen M et al. An automatic genetic algorithm framework for the optimization of three-dimensional surgical plans of forearm corrective osteotomies. Med Image Anal. 2020, 60: 101598.

Cerezal L, del Piñal F, Abascal F, García-Valtuille R, Pereda T, Canga A. Imaging findings in ulnar-sided wrist impaction syndromes. Radiographics. 2002, 22: 105–21.

Chia DS, Lim YJ, Chew WY. Corrective osteotomy in forearm fracture malunion improves functional outcome in adults. J Hand Surg Eur Vol. 2011, 36: 102–6.

Christensen JB, Adams JP, Cho KO, Miller L. A study of the interosseous distance between the radius and ulna during rotation of the forearm. Anat Rec. 1968, 160: 261–71.

Colaris J, Reijman M, Allema JH et al. Angular malalignment as cause of limitation of forearm rotation: an analysis of prospectively collected data of both-bone forearm fractures in children. Injury. 2014a, 45: 955–9.

Colaris JW, Allema JH, Reijman M et al. Which factors affect limitation of pronation/supination after forearm fractures in children? A prospective multicentre study. Injury. 2014b, 45: 696–700.

Croitoru H, Ellis RE, Prihar R, Small CF, Pichora DR. Fixation-based surgery: a new technique for distal radius osteotomy. Comput Aided Surg. 2001, 6: 160–9.

Dennler C, Bauer DE, Scheibler AG et al. Augmented reality in the operating room: a clinical feasibility study. BMC Musculoskelet Disord. 2021, 22: 451.

Dumont CE, Thalmann R, Macy JC. The effect of rotational malunion of the radius and the ulna on supination and pronation. J Bone Joint Surg Br. 2002, 84: 1070–4.

Fuller DJ, McCullough CJ. Malunited fractures of the forearm in children. J Bone Joint Surg Br. 1982, 64: 364–7.

Furrer PR, Kabelitz M, Schweizer A. Quantification of malalignment and corrective osteotomies in patients with malunion

after elastic stable intramedullary nailing of pediatric forearm fractures. J Hand Surg Glob Online. 2023, 5: 332–7.
Graham TJ, Fischer TJ, Hotchkiss RN, Kleinman WB. Disorders of the forearm axis. Hand Clin. 1998, 14: 305–16.
Honigmann P, Hofer M, Hirsch S et al. Cold ablation robot-guided laser osteotomy in hand, wrist and forearm surgery – a feasibility study. Int J Med Robot. 2022, 18: e2438.
Hreha J, Congiusta DV, Ahmed IH, Vosbikian MM. What is the normal ulnar bow in adult patients? Clin Orthop Relat Res. 2020, 478: 136–41.
Jupiter JB, Ruder J, Roth DA. Computer-generated bone models in the planning of osteotomy of multidirectional distal radius malunions. J Hand Surg Am. 1992, 17: 406–15.
Kasten P, Krefft M, Hesselbach J, Weinberg AM. How does torsional deformity of the radial shaft influence the rotation of the forearm? A biomechanical study. J Orthop Trauma. 2003, 17: 57–60.
Kataoka T, Oka K, Murase T. Rotational corrective osteotomy for malunited distal diaphyseal radius fractures in children and adolescents. J Hand Surg Am. 2018, 43: 286.e1–e8.
King GJ, McMurtry RY, Rubenstein JD, Gertzbein SD. Kinematics of the distal radioulnar joint. J Hand Surg Am. 1986, 11: 798–804.
Langenberg LC, Beumer A, The B, Koenraadt K, Eygendaal D. Surgical treatment of chronic anterior radial head dislocations in missed monteggia lesions in children: a rationale for treatment and pearls and pitfalls of surgery. Shoulder Elbow. 2020, 12: 422–31.
Lex JR, Koucheki R, Toor J, Backstein DJ. Clinical applications of augmented reality in orthopaedic surgery: a comprehensive narrative review. Int Orthop. 2023, 47: 375–91.
Lundskog J. Heat and bone tissue. An experimental investigation of the thermal properties of bone and threshold levels for thermal injury. Scand J Plast Reconstr Surg. 1972, 9: 1–80.
Mania S, Zindel C, Götschi T, Carrillo F, Fürnstahl P, Schweizer A. Malunion deformity of the forearm: three-dimensional length variation of interosseous membrane and bone collision. J Orthop Res. 2023, 41: 727–36.
Matthews LS, Kaufer H, Garver DF, Sonstegard DA. The effect on supination–pronation of angular malalignment of fractures of both bones of the forearm. J Bone Joint Surg Am. 1982, 64: 14–17.
Meesters AML, Assink N, FFA IJ. Functional outcome of 2-D- and 3-D-guided corrective forearm osteotomies: a systematic review. J Hand Surg Eur Vol. 2024, 49: 843–51.
Miyake J, Murase T, Oka K, Moritomo H, Sugamoto K, Yoshikawa H. Computer-assisted corrective osteotomy for malunited diaphyseal forearm fractures. J Bone Joint Surg Am. 2012, 94: e150.
Moritomo H, Noda K, Goto A, Murase T, Yoshikawa H, Sugamoto K. Interosseous membrane of the forearm: Length change of ligaments during forearm rotation. J Hand Surg Am. 2009, 34: 685–91.
Murase T, Oka K, Moritomo H, Goto A, Yoshikawa H, Sugamoto K. Three-dimensional corrective osteotomy of malunited fractures of the upper extremity with use of a computer simulation system. J Bone Joint Surg Am. 2008, 90: 2375–89.
Nagy L, Jankauskas L, Dumont CE. Correction of forearm malunion guided by the preoperative complaint. Clin Orthop Relat Res. 2008, 466: 1419–28.
Nishiwaki M, Welsh MF, Gammon B, Ferreira LM, Johnson JA, King GJ. Effect of volarly angulated distal radius fractures on forearm rotation and distal radioulnar joint kinematics. J Hand Surg Am. 2015, 40: 2236–42.
Noda K, Goto A, Murase T, Sugamoto K, Yoshikawa H, Moritomo H. Interosseous membrane of the forearm: An anatomical study of ligament attachment locations. J Hand Surg Am. 2009, 34: 415–22.
Oka K, Tanaka H, Okada K et al. Three-dimensional corrective osteotomy for malunited fractures of the upper extremity using patient-matched instruments: a prospective, multicenter, open-label, single-arm trial. J Bone Joint Surg Am. 2019, 101: 710–21.
Price CT, Knapp DR. Osteotomy for malunited forearm shaft fractures in children. J Pediatr Orthop. 2006, 26: 193–6.
Ries M, O'Neill D. A method to determine the true angulation of long bone deformity. Clin Orthop Relat Res. 1987: 191–4.
Robinson L, Shatford R. Anatomy of the forearm. In: Gupta A (Ed.) The Grasping Hand: Structural and Functional Anatomy of the Hand and Upper Extremity. Thieme, 2021.
Roner S, Vlachopoulos L, Nagy L, Schweizer A, Fürnstahl P. Accuracy and early clinical outcome of 3-dimensional planned and guided single-cut osteotomies of malunited forearm bones. J Hand Surg Am. 2017, 42: 1031.e1–e8.
Roth KC, Walenkamp MMJ, van Geenen RCI, Reijman M, Verhaar JAN, Colaris JW. Factors determining outcome of corrective osteotomy for malunited paediatric forearm fractures: a systematic review and meta-analysis. J Hand Surg Eur Vol. 2017, 42: 810–6.
Roth K, van Es E, Kraan G, Eygendaal D, Colaris J, Stockmans F. Accuracy of 3D corrective osteotomy for pediatric malunited both-bone forearm fractures. Children (Basel). 2022, 10: 21.
Rouleau DM, Faber KJ, Athwal GS. The proximal ulna dorsal angulation: a radiographic study. J Shoulder Elbow Surg. 2010, 19: 26–30.
Rupasinghe SL, Poon PC. Radius morphology and its effects on rotation with contoured and noncontoured plating of the proximal radius. J Shoulder Elbow Surg. 2012, 21: 568–73.
Sangeorzan BP, Judd RP, Sangeorzan BJ. Mathematical analysis of single-cut osteotomy for complex long bone deformity. J Biomech. 1989, 22: 1271–8.
Schmitt S, Eisa A, Radosavljevic J, van Schoonhoven J. Dynamic palmar dislocation of the ulnar head at the distal radioulnar joint (druj) after radius shaft malunion. Arch Orthop Trauma Surg. 2023, 143: 2781–7.
Shiode R, Miyamura S, Kazui A et al. Acceptable range of forearm deformity derived from relation to three-dimensional analysis and clinical impairments. J Orthop Res. 2024, 42: 1509–18.
Tarr RR, Garfinkel AI, Sarmiento A. The effects of angular and rotational deformities of both bones of the forearm. An in vitro study. J Bone Joint Surg Am. 1984, 66: 65–70.
Trousdale RT, Linscheid RL. Operative treatment of malunited fractures of the forearm. J Bone Joint Surg Am. 1995, 77: 894–902.
Vlachopoulos L, Schweizer A, Graf M, Nagy L, Fürnstahl P. Three-dimensional postoperative accuracy of extra-articular forearm osteotomies using CT-scan based patient-specific surgical guides. BMC Musculoskelet Disord. 2015, 16: 336.
von Campe A, Nagy L, Arbab D, Dumont CE. Corrective osteotomies in malunions of the distal radius: do we get what we planned? Clin Orthop Relat Res. 2006, 450: 179–85.
Vroemen JC, Dobbe JG, Strackee SD, Streekstra GJ. Positioning evaluation of corrective osteotomy for the malunited radius: 3-D CT versus 2-D radiographs. Orthopedics. 2013, 36: e193–9.
Weber MB, Olgun ZD, Boden KA et al. A cadaveric study of radial and ulnar bowing in the sagittal and coronal planes. J Shoulder Elbow Surg. 2020, 29: 1010–8.